Spin-domain formation in antiferromagnetic condensates

Michal Matuszewski, Tristram J. Alexander, and Yuri S. Kivshar
Nonlinear Physics Center and ARC Center of Excellence for Quantum-Atom Optics, Research School of Physical Sciences and Engineering, Australian National University, Canberra ACT 0200, Australia
(Received 29 February 2008; published 27 August 2008)

Antiferromagnetic condensates are generally believed not to display modulational instability and subsequent spin-domain formation. Here we demonstrate that in the presence of a homogeneous magnetic field antiferromagnetic spin-1 Bose-Einstein condensates can undergo spatial modulational instability followed by the subsequent generation of spin domains. Employing numerical simulations for realistic conditions, we show how this effect can be observed in sodium condensates confined in an optical trap. Finally, we link this instability and spin-domain formation with stationary modes of the condensate.

DOI: 10.1103/PhysRevA.78.023632 PACS number(s): 03.75.Lm, 05.45.Yv

I. INTRODUCTION

The appearance of spin degrees of freedom in atomic matter waves opens up possibilities for different phenomena such as spin waves [1], spontaneous magnetization [2], and spin mixing [3]. However, perhaps the most intriguing effect is associated with complex patterns, such as spin textures [4] or domains [5], which may appear either as stationary low-energy states or emerge spontaneously due to condensate instabilities. Pattern formation is a common feature in the dynamics of extended nonlinear systems ranging from optics [6] to fluids [7]. Such patterns often develop through the exponential growth of unstable spatial modulations, known as *modulational instability*. In the spinor condensates we have the opportunity to examine such effects in an environment which is remarkably easy to control and manipulate, simply through the addition of an external magnetic field.

The origin of the intriguing physics of spinor condensates lies in the spin interaction between atoms, which allows for an exchange of atoms between different spin components. The parametric nature of this interaction mirrors similar effects observed in nonlinear optics, where the interaction of several optical modes may lead to the generation of different frequencies [6]. Of particular interest to our case is the possibility that instabilities of an intense light beam may occur even when the wave is coupled to a spatially stable eigenmode and propagates in the normal-dispersion regime [8]; in this case, the interplay of natural and self-induced birefringence leads to nonlinear polarization symmetry breaking and *polarization modulational instability*. By analogy, we thus might expect similar instabilities in an initially stable polar condensate subjected to additional spin component coupling through an external magnetic field.

In the absence of an external magnetic field, the development of spatial modulational instability in three-component (or spin-1) *ferromagnetic* condensates and the subsequent formation of spin domains has been well established both theoretically [9–11] and experimentally [12]. However, early work on the zero-field case [9] determined that antiferromagnetic (or polar) condensates are *modulationally stable*. Experimental observations suggested this is also true for a weak magnetic field; however, these experiments were carried out with a condensate smaller than a spin domain [13].

In this paper we reveal that in fact the presence of a weak magnetic field ($\sim$175 mG) leads to spin-domain formation in antiferromagnetic condensates, provided the condensate is larger than the spin healing length. Furthermore, we show that this spin-domain formation is initiated by a *novel type of modulational instability*, reminiscent of instabilities observed in nonlinear optics [8] and not seen before in Bose-Einstein condensates. While spin-domain formation in antiferromagnetic condensates has been observed before in the presence of a magnetic field gradient [5], we show here that it occurs equally well in the presence of a homogeneous magnetic field. Furthermore, we reveal that this modulational instability and spontaneous spin-domain formation is associated with stationary states which exist in the presence of a weak magnetic field and which intrinsically break the validity of the single-mode approximation (as seen earlier in [14]). We discuss realistic experimental conditions for the observation of these effects.

The paper is organized as follows. Section II introduces the theoretical model of spin-1 condensates in a homogeneous magnetic field. In Sec. III we investigate homogeneous stationary states in a magnetic field and analyze their stability with respect to plane-wave perturbations (modulational stability). Section IV presents results of numerical simulations corresponding to experimentally relevant condensate evolution, demonstrating the possibility of the observation of instability in an antiferromagnetic condensate. In Sec. V we link this instability and spin-domain formation with stationary modes of the condensate, and Sec. VI concludes the paper.

II. MODEL

The evolution of a dilute spin-1 ($F=1$) Bose-Einstein condensate (BEC) in a homogeneous magnetic field is given by the coupled Gross-Pitaevskii equations (GPEs)

$$i\hbar\frac{\partial\Psi_{\pm}}{\partial t}=[\mathcal{L}+\tilde{c}_2(n_{\pm}+n_0-n_{\mp})]\Psi_{\pm}+\tilde{c}_2\Psi_0^2\Psi_{\mp}^*,$$

$$i\hbar\frac{\partial\Psi_0}{\partial t}=[\mathcal{L}-\delta E+\tilde{c}_2(n_++n_-)]\Psi_0+2\tilde{c}_2\Psi_+\Psi_-\Psi_0^*, \quad (1)$$

where $\mathcal{L}=-\hbar^2\nabla^2/2m+\tilde{c}_0n+V(\mathbf{r})$, $n_j=|\Psi_j|^2$, $n=n_++n_0+n_-$, and $V(\mathbf{r})$ is an external potential. The nonlinear coefficients

are $\tilde{c}_0=4\pi\hbar^2(2a_2+a_0)/3m$ and $\tilde{c}_2=4\pi\hbar^2(a_2-a_0)/3m$. The total number of atoms, $N=\int|n(\mathbf{r})|^2d\mathbf{r}$, and the total magnetization $M=\int[|n_+(\mathbf{r})|^2-|n_-(\mathbf{r})|^2]d\mathbf{r}$ are conserved quantities. The Zeeman-energy shifts for each component can be calculated using the Breit-Rabi formula [15]

$$E_\pm=-\frac{1}{8}E_{\mathrm{HFS}}(1+4\sqrt{1\pm\alpha+\alpha^2})\mp g_I\mu_B B,$$

$$E_0=-\frac{1}{8}E_{\mathrm{HFS}}(1+4\sqrt{1+\alpha^2}), \tag{2}$$

where E_{HFS} is the hyperfine energy splitting at zero magnetic field and $\alpha=(g_I+g_J)\mu_B B/E_{\mathrm{HFS}}$, where μ_B is the Bohr magneton, and g_I and g_J are the gyromagnetic ratios of electron and nucleus. The linear part of the Zeeman effect does not affect the condensate evolution, except for a change in the relative phases [16], and so we remove it with the transformation $\Psi_\pm\rightarrow\Psi_\pm\exp(-iE_\pm t)$, $\Psi_0\rightarrow\Psi_0\exp[-i(E_++E_-)t/2]$. We thus consider only the effects of the quadratic Zeeman shift, $\delta E=(E_++E_--2E_0)/2\approx\alpha^2E_{\mathrm{HFS}}/16$, which is always positive.

III. MODULATIONAL INSTABILITY OF HOMOGENEOUS STATIONARY STATES

First, we are interested in the stability analysis of the homogeneous condensate and consider the case of vanishing potential, $V(\mathbf{r})=0$. We look for the homogeneous solutions in the form $\psi_j=\sqrt{n_j}e^{-i\mu_j t+i\theta_j}$. The "phase-matching condition" for Eqs. (1) gives $\mu_++\mu_-=2\mu_0$. We find that both in the case of $B=0$ and in the case of $M=0$, the steady state fulfills the stronger condition $\mu_+=\mu_-=\mu_0$. However, if both magnetic field and magnetization are nonzero, which is the case in real experiments, the chemical potentials will be different, satisfying the less stringent phase-matching condition.

We define the density fraction in each component as $\rho_j=n_j/n$. If we assume that all three spin components ρ_j are nonvanishing, the relative phase between them, $\theta=2\theta_0-\theta_+-\theta_-$, can take the value 0 or π only. We will describe the corresponding stationary states as phase-matched ($\theta=0$) and anti-phase-matched ($\theta=\pi$). Note that both types of states can in general exist in both ferromagnetic and polar condensates [16–18]. However, phase-matched states are energetically favorable in ferromagnetic condensates and anti-phase-matched states in polar condensates [14,16]. For that reason, they were named ferromagnetic and polar states, respectively, in Ref. [16]. In Fig. 1 we present the existence diagram for three-component homogeneous stationary states. For generality we also include the results for ferromagnetic condensates. The ferromagnetic condensates, such as ^{87}Rb, occur in the lower half (where c_2 is negative), while polar condensates, such as ^{23}Na, occur in the upper half (c_2 is positive). There is clearly a region of coexistence of anti-phase-matched (APM) and phase-matched (PM) states for a polar condensate in nonzero magnetic field. In addition, a two-component solution with $\rho_0=0$ and one-component solutions with $\rho_j=1$ exist. Our results are in agreement with a previous analysis of homogeneous ground states [14].

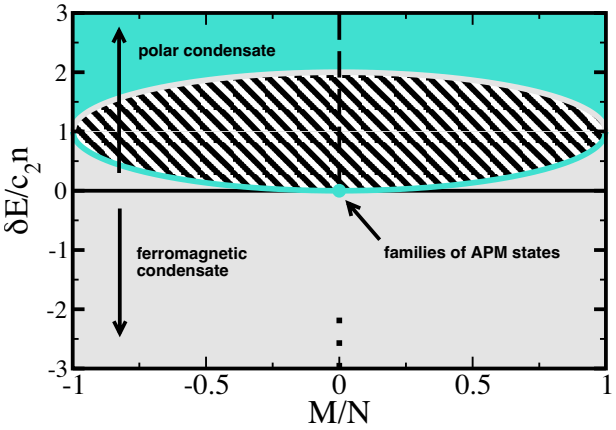

FIG. 1. (Color online) Diagram of existence of stationary states in spin-1 condensates. In addition to the three-component phase-matched and anti-phase-matched solutions shown in the diagram, two-component solutions with $\rho_0=0$ exist for arbitrary M and one-component solutions $\rho_j=1$ exist with $j=-,0,+$. Dark shading (top), anti-phase-matched state; light shading (bottom), phase-matched state; cross hatching, both states. The dotted and dashed lines at $M=0$ indicate the absence of a phase-matched or anti-phase-matched state, respectively.

The energy density is related to the Hamiltonian of the system, from which Eqs. (1) are derived, by $H=\int E\,d\mathbf{r}$. In addition to the anti-phase-matched ground state [14], the polar condensate in the coexistence region of Fig. 1 has an excited phase-matched state corresponding to the energy maximum at $\theta=0$. This state is stable with respect to spatially homogeneous spin mixing, because the possible dynamical trajectories in the (ρ_0,θ) plane correspond to a constant energy value; hence, both minima and maxima are stable.

The stability properties of these states change when we consider the possibility of a spatial, or modulational, instability (MI). We calculate the growth rate of the Bogoliubov modes [19]:

$$\psi_j=[\sqrt{n_j}+u_j(t)e^{i\mathbf{k}\cdot\mathbf{x}}+v_j^*(t)e^{-i\mathbf{k}\cdot\mathbf{x}}]e^{-i\mu_j t+i\theta_j}. \tag{3}$$

After substituting the above into Eq. (1) we obtain a set of equations for the vector $\mathbf{z}=(u_+,u_0,u_-,v_+^*,v_0^*,v_-^*)$ in the form $d\mathbf{z}/dt=iA\mathbf{z}$, where A is a sixth-rank matrix [20]. For an equilibrium state, it is possible to eliminate μ_j and δE from A, expressing it in terms of n_j, c_0, c_2, and k only for specific θ. The Bogoliubov modes are the solutions of the characteristic equation $\det(A-\hbar\omega)=0$, with ω being the eigenfrequency of the excitation. The form of this equation is too cumbersome to present here, in contrast to the $B=0$ case considered before [11]. In general, one has to use numerical methods to obtain a set of solutions.

The general numerical results are presented in a systematic way in Table I. These results have been calculated for the specific cases of the ^{87}Rb condensate (upper half) and ^{23}Na condensate (lower half) with scattering lengths given in [16] and hyperfine energy splitting given in [21]. As we are considering the homogeneous case, the result is applicable to one-, two-, and three-dimensional condensates. We do not

TABLE I. Stability of spin-1 condensate states in the absence and presence of the magnetic field: PM, phase-matched; APM, anti-phase-matched; X, state does not exist.

Condensate type	State type	$B=0$ $M=0$	$B=0$ $M\neq 0$	$B\neq 0$ $M=0$	$B\neq 0$ $M\neq 0$
Ferro	PM	Stable	Stable	Stable	Stable
	APM	Unstable[a]	X	X	X
	$\rho_0=0$	Unstable	Unstable	Unstable	Unstable
	$\rho_0=1$	Unstable	X	Unstable	X
Polar	PM	Stable	Stable	Unstable	Unstable
	APM	Stable[a,b]	X	X	Unstable
	$\rho_0=0$	Stable	Stable	Unstable	Unstable
	$\rho_0=1$	Stable	X	Stable	X

[a]A family of stationary states.
[b]Neutral stability with respect to spatially homogeneous spin mixing.

consider here the trivial case of $\rho_\pm=1$ states, which have an extremal value of magnetization of $M=\pm N$. All the cases presented in this table were double checked by direct numerical integration of Eq. (4) (see Sec. IV). The results cover the area of Fig. 1 and do not apply to the case of very high magnetic field, when the quadratic Zeeman energy dominates.

We find that our results are in agreement with the existing data for the vanishing magnetic field case. In Ref. [9] the authors found that all the three-component equilibrium states are stable, with the exception of one state in the ferromagnetic condensate, which corresponds to the "ferro-APM," $M=0$ state in Table I. In Ref. [16], it was also found that ground states of both ferromagnetic and polar condensates ("ferro-PM" and "polar-APM") are modulationally stable. The authors of Ref. [11] considered mainly non equilibrium (spin-mixing) states, but their general conclusion was that all polar condensate states are dynamically stable and ferromagnetic are not. Here we report that, in fact, specific ferromagnetic condensate states are stable, while polar condensates may become unstable. Furthermore, as discussed below, we see that dynamic domain formation may occur for polar condensates and lead to convergence to different stationary states.

As one can see in Table I, the magnetic field affects the stability of polar condensates. We investigate this phenomenon in detail by calculating the growth rate $\kappa=\mathrm{Im}(\omega)$ corresponding to unstable Bogoliubov modes. In Fig. 2, we present results for a "polar-PM" state of a sodium condensate as a function of the magnetic field strength. The growth rate is proportional to the square of the quadratic Zeeman shift, which is in turn proportional to the square of the magnetic field strength. Hence, one has to apply a *relatively strong magnetic field* to observe MI on a reasonable time scale. Another interesting feature is the range of wave vectors k corresponding to unstable modes. In contrast to the typical case where this range starts from $k=0$, here the unstable region begins at a nonzero minimum value. This type of "optical mode" branch has been reported before in the case of parametric optical solitons [20].

IV. DYNAMICS OF THE CONDENSATE IN A CIGAR-SHAPED TRAP

We now consider the implications of these results in the experimentally relevant case of a ^{23}Na condensate localized in a cigar-shaped harmonic trap, $V(\mathbf{r})=\frac{1}{2}m\omega_\perp^2(y^2+z^2)+\frac{1}{2}m\omega_\parallel^2x^2$. Specifically we consider the case $\omega_\perp \gg \omega_\parallel$ in which the Fermi radius of the transverse trapping potential is smaller than the spin healing length and the nonlinear energy scale is much smaller than the transverse trap energy scale, which allows us to reduce the problem to one spatial dimension [16,22]. Following the standard dimensionality reduction procedure we obtain the one-dimensional model

$$i\hbar\frac{\partial\psi_\pm}{\partial t}=[\tilde{\mathcal{L}}+c_2(n_\pm+n_0-n_\mp)]\psi_\pm+c_2\psi_0^2\psi_\mp^*,$$

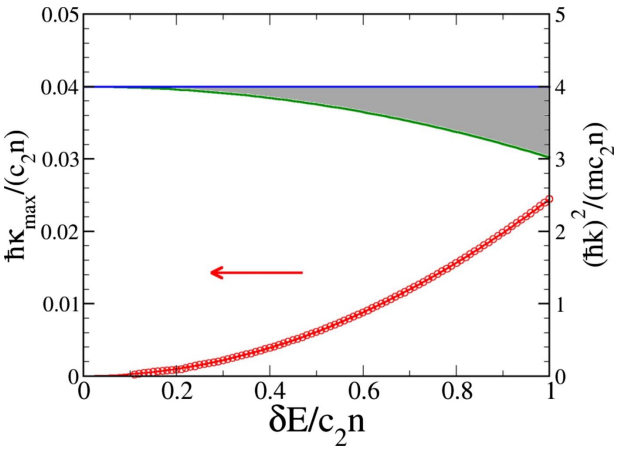

FIG. 2. (Color online) Modulational instability growth rate in a phase-matched steady state of a sodium condensate (circles) versus the quadratic Zeeman shift in the case $M=0$. The solid line is a square fit to the numerical data. The upper shaded area shows the range of k vectors corresponding to the unstable (imaginary) frequencies.

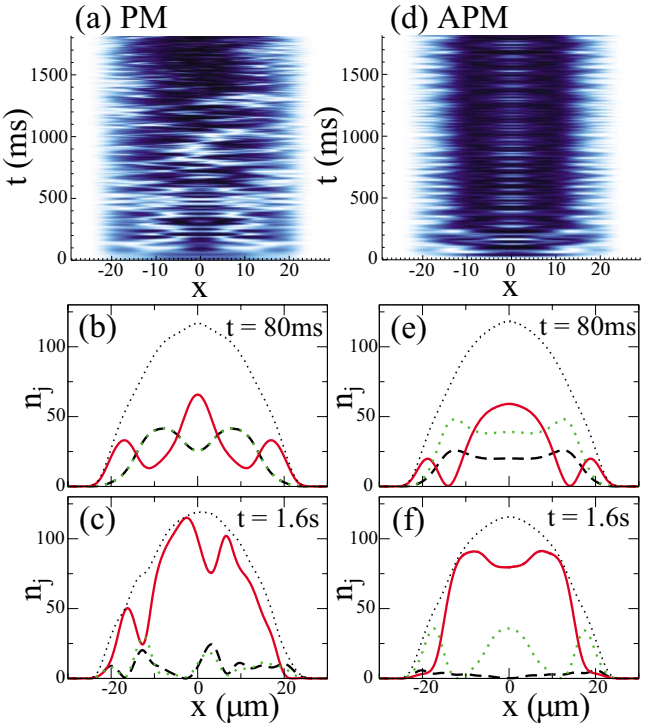

FIG. 3. (Color online) Spin-domain formation in a ^{23}Na condensate confined in an optical harmonic trap. Top panels: evolution of n_0 (darker shading higher density). Bottom panels: densities at given times. (a), (b), (c) Phase-matched initial state, $\rho_{+,0,-}=0.351,0.3,0.349$; (d), (e), (f) anti-phase-matched initial state, $\rho_{+,0,-}=0.4,0.01,0.59$. The thin dotted line corresponds to the total condensate density n, and the dashed, solid, and dotted lines correspond to n_+, n_0, and n_-, respectively. Parameters are $N=3.7\times10^3$, $B=175$ mG, $\omega_\perp=2\pi\times10^3$ Hz, and $\omega_\parallel=2\pi\times32$ Hz.

$$i\hbar\frac{\partial\psi_0}{\partial t}=[\tilde{\mathcal{L}}-\delta E+c_2(n_++n_-)]\psi_0+2c_2\psi_+\psi_-\psi_0^*, \quad (4)$$

where $\tilde{\mathcal{L}}=-(\hbar^2/2m)\partial^2/\partial x^2+c_0n+\frac{1}{2}m\omega_\parallel^2x^2$ and the interaction coefficients have been rescaled and now include the transverse trap frequency: $c_0=4\hbar\omega_\perp(2a_2+a_0)/3$ and $c_2=4\hbar\omega_\perp(a_2-a_0)/3$.

The experimental scenario we consider here consists of several phases. Initially, the condensate is prepared in the $m=-1$ ground state [12]. Next, short microwave field pulses are applied to transfer the atomic population to the desired state [23]. We consider two cases: a phase-matched state ($\theta=0$) with $\rho_{+,0,-}=0.351,0.3,0.349$ and an anti-phase-matched state ($\theta=\pi$) with $\rho_{+,0,-}=0.4,0.01,0.59$. Simultaneously, the magnetic field is set to the value of 175 mG [12]. The results of the corresponding numerical simulations of Eqs. (4) are presented in Fig. 3. The MI develops after tens of milliseconds and leads rapidly to spin-domain formation. We see what appears to be initial oscillations, followed by instability dynamics, leading to an apparent oscillating state. In the case of the phase-matched initial condition and almost zero magnetization, we ultimately see conversion to the ψ_0 component, as observed in experiment [13]. In the anti-phase-matched initial condition, however, with nonzero magnetization, the spin domains become well defined and persist in the dynamics. We have verified that the nonlinear energy at peak density $c_0n_{\max}/2$ is much smaller than the transverse energy separation $\hbar\omega_\perp$, which justifies the use of a reduced one-dimensional GPE [22].

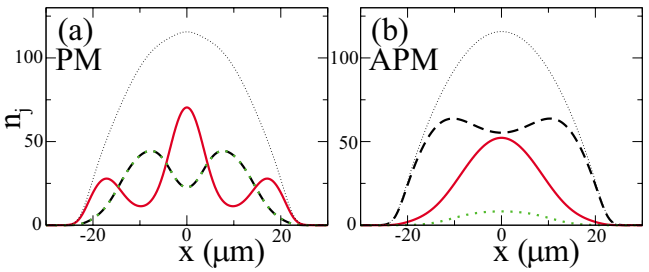

FIG. 4. (Color online) Examples of (a) phase-matched and (b) anti-phase-matched stationary states in a ^{23}Na condensate. Shown are the total density n (thin dotted line) and component densities $n_{+,0,-}$ (dashed, solid, and dotted lines, respectively).

V. STATIONARY SPINOR STATES

The existence of MI suggests that domain-type stationary states may be expected in the trap, just as plane-wave instability and solitons are typically found together in optics. Indeed, as can be seen in Fig. 4, we find that in the stationary picture the profiles always break the single-mode approximation for both the phase-matched and anti-phase-matched states (as found in Ref. [14] for the case of an anti-phase-matched state in a polar condensate). As predicted by the MI analysis, an initially smooth profile will therefore become modulated with the ensuing instability dynamics reflecting the nearby stationary-state profiles. For instance, comparing Figs. 3(b) and 4(a) we see that profiles similar to the stationary states appear in the evolution. Significantly, but unsurprisingly, in a polar condensate, we find that the phase-matched state is generally unstable, while the anti-phase-matched state is stable. The stability of these states appears to reflect the ultimate dynamics of the condensate with the phase-matched state breaking up while the anti-phase-matched state has highly persistent spin domains. A complete analysis of the stability of the stationary states will be presented elsewhere.

VI. CONCLUSIONS

We have demonstrated that an antiferromagnetic spin-1 condensate can undergo a different type of spatial modulational instability followed by subsequent spin-domain formation in the presence of a homogeneous magnetic field. We have employed realistic conditions to demonstrate, with the help of numerical simulations, that this modulational instability can be observed in a sodium condensate confined in an optical trap potential and that the ensuing instability dynamics connect with the stationary states in the trap.

ACKNOWLEDGMENTS

This work was supported by the Australian Research Council through the ARC Discovery Project and Centre of Excellence for Quantum-Atom Optics. M.M. acknowledges support from the Foundation for Polish Science.

[1] T.-L. Ho, Phys. Rev. Lett. **81**, 742 (1998).
[2] J. M. Higbie, L. E. Sadler, S. Inouye, A. P. Chikkatur, S. R. Leslie, K. L. Moore, V. Savalli, and D. M. Stamper-Kurn, Phys. Rev. Lett. **95**, 050401 (2005).
[3] M.-S. Chang, C. D. Hamley, M. D. Barrett, J. A. Sauer, K. M. Fortier, W. Zhang, L. You, and M. S. Chapman, Phys. Rev. Lett. **92**, 140403 (2004).
[4] A. E. Leanhardt, Y. Shin, D. Kielpinski, D. E. Pritchard, and W. Ketterle, Phys. Rev. Lett. **90**, 140403 (2003).
[5] J. Stenger, S. Inouye, D. M. Stamper-Kurn, H.-J. Miesner, A. P. Chikkatur, and W. Ketterle, Nature (London) **396**, 345 (1998).
[6] R. W. Boyd, *Nonlinear Optics* (Academic Press, San Diego, 2002).
[7] See, e.g., M. C. Cross and P. C. Hohenberg, Rev. Mod. Phys. **65**, 851 (1993).
[8] G. Millot, E. Seve, and S. Wabnitz, Phys. Rev. Lett. **79**, 661 (1997).
[9] N. P. Robins, W. Zhang, E. A. Ostrovskaya, and Y. S. Kivshar, Phys. Rev. A **64**, 021601(R) (2001).
[10] H. Saito and M. Ueda, Phys. Rev. A **72**, 023610 (2005).
[11] W. Zhang, D. L. Zhou, M.-S. Chang, M. S. Chapman, and L. You, Phys. Rev. Lett. **95**, 180403 (2005).
[12] L. E. Sadler, J. M. Higbie, S. R. Leslie, M. Vengalattore, and D. M. Stamper-Kurn, Nature (London) **443**, 312 (2006).
[13] A. T. Black, E. Gomez, L. D. Turner, S. Jung, and P. D. Lett, Phys. Rev. Lett. **99**, 070403 (2007).
[14] W. X. Zhang, S. Yi, and L. You, New J. Phys. **5**, 77 (2003).
[15] S. Wüster, T. E. Argue, and C. M. Savage, Phys. Rev. A **72**, 043616 (2005).
[16] B. J. Dąbrowska-Wüster, E. A. Ostrovskaya, T. J. Alexander, and Y. S. Kivshar, Phys. Rev. A **75**, 023617 (2007).
[17] D. R. Romano and E. J. V. de Passos, Phys. Rev. A **70**, 043614 (2004).
[18] H. E. Nistazakis, D. J. Frantzeskakis, P. G. Kevrekidis, B. A. Malomed, R. Carretero-Gonzalez, and A. R. Bishop, Phys. Rev. A **76**, 063603 (2007).
[19] A. Smerzi and A. Trombettoni, Phys. Rev. A **68**, 023613 (2003).
[20] S. Trillo and P. Ferro, Opt. Lett. **20**, 438 (1995).
[21] E. Arimondo, M. Inguscio, and P. Violino, Rev. Mod. Phys. **49**, 31 (1977).
[22] L. Salasnich, A. Parola, and L. Reatto, Phys. Rev. A **65**, 043614 (2002); W. Zhang and L. You, *ibid.* **71**, 025603 (2005).
[23] J. Kronjäger, C. Becker, M. Brinkmann, R. Walser, P. Navez, K. Bongs, and K. Sengstock, Phys. Rev. A **72**, 063619 (2005).